RSC Advances

Journal Name

RSC Advances

ARTICLE TYPE

The Sensitive and Efficient Trifluoroacetyl-based Aromatic Fluorescent Probe for Organic Amine Vapour Detection

JunjunYao[a,b], Yanyan Fu [a], Wei Xu [a], Tianchi Fan[a,b], Qingguo He[a] *, Defeng Zhu [a], Huimin Cao [a] and Jiangong Cheng [a] *

Volatile organic amines can induce a number of deleterious effects on the ecological environment and human health. A highly efficient detection method is in exigent need. A series of fluorescent probes with trifluoroacetyl as reactive unit and aromatic moieties including anthracene (**ANT-TFA**), pyrene (**PY-TFA**) and triphenylamine (**TPA-TFA**) unit as fluorophore have been designed for highly reversible, sensitive and efficient amine detection in this contribution. The aromatic unit could significantly tune the reactivity and fluorescent property of the probe. A rapid, reversible and sensitive (ppm to sub-ppb) probe could be realized for differentiating of primary and secondary alkyl amines and aniline. Materials Studio was used for understanding the reactivity and sensing performance difference. The findings reported 15 herein can greatly advance the real-time monitoring and differentiating of trace organic amines.

1.Introduction

Organic amine is one of the sources of grievous social and health problems owing to the fact that organic amines widely exist in the pharmaceutical factories, chemical plants, tanneries, meat food 20 processing plants, dustbins, sewers, initiating acute or delayed toxicities to human skins, respiratory systems, nervous systems, urinary systems, hematopoietic systems, etc.[1, 2] And thus, a high sensitive and selective detection method for the determination and discrimination of trace volatile organic amines is in exigent 25 need.

Fluorescent sensors have attracted a considerable interest in recent years because of their higher sensitivity, higher selectivity and lower detection limit.[3-11] Lu et al. reported a sensitive and discriminative fluorescent chemosensor for aliphatic amines via a 30 readily detectable excited-state complex, but the probe cannot detect aromatic amines.[12] Tang et al. reported a sensitive and selective fluorescence-switchable luminogen sensor for the fast "turn-on'' detection of primary amine gas.[13] Swager et al. reported that the fluorescence of conjugated cationic fluorescent 35 polymers with various anions, was found to be instantaneously quenched by volatile amines vapour at a ppm concentration.[14]

Despite prominent successes of amine fluorescent chemosenors, there are still some issues to be addressed. For example, firstly, the design and synthesis of probe materials may 40 require redundant experimental procedures, it was reported that the synthesis of Zimmerman's cross-linked dendrimer imprinted polymer for amine guests is up to 12 steps,[15] which would restrict the practical application. Secondly, lots of existing probe materials cannot realize multi-stage amine detection.[16, 17] Thirdly, 45 many detection methods based on chemical reaction,[18,19] between the fluorescent probe materials and amines are irreversible, which

may produce additional cost for application.

In this contribution, we aimed to obtain a simple and multi-stage amine fluorescent probe that could realize a rapid and 50 reversible response capable for real-time and onsite monitoring of organic amine pollutants.

Trifluoroacetyl group was chosen as the functional unit for reversibly reacting with a series of amines to form hemiaminals or zwitterions[20-22](Figure S1). And one suitable aromatic unit 55 should be adopt as the fluorophore. As known for an excellent fluorescent probe, the structure including rigidity, size, conformation and electron donating ability of the aromatic unit will highly influence the fluorescent properties and the reactivity, and hence will influence the sensing performance. Here, 60 anthracene, pyrene and triphenylamine were selected to connect with trifluoroacetyl, respectively. From anthracene to pyrene, the size of the aromatic ring will be enlarged, and triphenamine is different with anthracene and pyrene in that it shows a pyramidal conformation which will show a quite different fluorescent 65 property especially in solid state in preventing intermolecular interaction. And for simplification, they are named **ANT-TFA**, **PY-TFA** and **TPA-TFA** according to the aromatic ring anthracene, pyrene and triphenylamine respectively. Their chemical structures are shown in Figure 1.
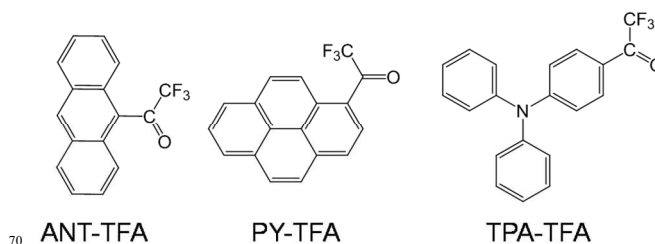

70 Figure 1.Chemical structures of **ANT-TFA**, **PY-TFA**, **TPA-TFA**.

In this contribution, the synthesis, optical property and sensing performance were investigated. The relationship of the molecular structure and the sensing performance was discussed. It is found that **PY-TFA** and **TPA-TFA** showed excellent reversibility, quick response, sensitivity to aliphatic primary and secondary amine vapour at low ppm-ppb detection limit, **TPA-TFA** even could detect aniline with a detection limit of 0.23 ppb.

2.Experimental Section

2.1Materials and Measurements

All chemicals were purchased from commercial sources and were used as received without any further purification except especial instruction. All organic solvents and amines used were of analytical grade. The sensing films were prepared by spin-coating a tetrahydrofuran (THF) solution of each material onto a 10×20 mm quartz plate by KW-4A spin coater based desktop at 2000 rpm and placed under vacuum for 30 minutes before use. The ^{1}H-NMR and ^{13}C-HMR spectra were recorded on a Bruker DRX500 instrument, and tetramethylsilane (TMS) was used as an internal standard. The MS spectra were measured by Bruker Daltonics Inc. APEXII FT-ICR MS. UV-Vis absorption and fluorescence analysis were achieved by a Jasco V-670 spectrophotometer and a Jasco FP 6500 spectrometer, respectively. Cyclic voltammetry (CV) experiments were accomplished by means of a CH Instruments electrochemical analyzer. Molecular simulations were carried on Materials Studio provided by the Accelrys America. All the theoretical calculations were performed by DMol3 program in the Materials Studio 7.0, which is one of the quantum mechanical code using density functional theory. BLYP function of generalized gradient approximation (GGA) level was used to calculate the optical absorption spectra and the energy level of the molecular orbital. The detail methodology and parameters are listed in Table S1 in the supporting information. .

2.2 Synthesis of ANT-TFA, PY-TFA,TPA-TFA

Scheme 1.Synthetic routes for R-TFA.
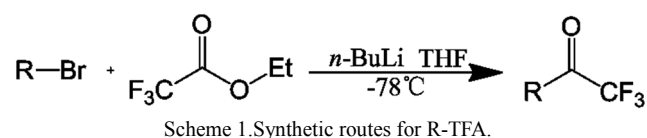
The synthetic procedure was demonstrated in Scheme 1. 9-bromoanthracene, 1-bromopyrene, 4-bromotriphenylamine were subjected to *n*-butyllithium solution under N_2 atmosphere at -78°C to remove the bromine, and the subsequent reaction with ethyl trifluoroacetate to acquire trifluoroacetyl–substituted derivatives, namely, **ANT-TFA**, **PY-TFA**, **TPA-TFA** with yields of 37%, 30% and 22%，respectively.

ANT-TFA: ^{1}H NMR (500MHZ, CDCl$_3$, ppm): δ 8.63(s, 1H), 8.08 (m, 2H), 7.76 (d, *J*=10.0Hz, 2H), 7.56(m, 4H). ^{13}C-NMR(125.7 MHz，CDCl$_3$，ppm):δ191.27, 130.91, 128.94, 128.13, 127.32, 125.86, 123.85, 117.14, 114.81. FT-ICR MS for C$_{16}$H$_9$F$_3$O calcd.: 274.0605；found: 274.0603.

PY-TFA: ^{1}H NMR (500MHz, CDCl$_3$, ppm): δ 9.10 (d, *J*=10.0Hz, 1H), 8.51 (m, 1H), 8.25 (m, 3H), 8.17 (d, *J*=10.0Hz, 1H), 8.08(m, 2H), 8.00 (d, *J*=10.0Hz, 1H). ^{13}C-NMR(125.7 MHz

，CDCl$_3$，ppm):δ182.76, 135.82, 132.24, 131.33, 130.78, 130.11, 128.17, 127.42, 127.12, 126.83, 124.87, 123.91, 123.75, 123.57, 122.24, 120.48, 118.15, 115.81. FT-ICR MS for C$_{18}$H$_9$F$_3$O calcd.: 298.0605; found:298.0602.

TPA-TFA: ^{1}H NMR (500M, CDCl$_3$, ppm): δ 7.87 (d, *J*=9.0Hz, 2H), 7.37 (m, 4H), 7.21 (m, 6H), 6.94 (d, *J*=9.0Hz, 2H). ^{13}C-NMR(125.7MHz，CDCl$_3$，ppm):δ 178.35, 154.05, 145.47, 132.04, 130.11, 129.24, 126.91,125.83, 124.35, 121.24, 118.33, 116.01. FT-ICR MS for C$_{20}$H$_{15}$F$_3$NO [M+H$^+$] calcd.: 342.1100; found:342.1104.

3.Results and Discussion

3.1Optical and Electrochemical Properties

Figure 2 demonstrates the absorption and emission spectra of the three probes in solution and film state. Table 1 summarizes the optical and electrochemical data. In THF solution, as Figure 2a shows, **TPA-TFA** has one strong absorption peak at 380 nm and two very weak peaks below 300 nm. **PY-TFA** has two strong absorption peaks at 376 and 410 nm and two very strong absorption peaks below 300 nm. While **ANT-TFA** has very weak absorption peaks within 300~400 nm, the main absorption peak is below 300 nm. According to a calculation based on DMol3 program at BLYP function of GGA level, the peaks larger than 300 nm here mentioned all come from a charge transfer (CT) state from the aromatic ring to TFA group (Figure S8~S10). Figure 2b exhibits that **TPA-TFA** has the longest emission at 543 nm, **PY-TFA** has one structureless emission band peaked at 444 nm, and **ANT-TFA** shows the shortest emission with fine structure. And in solution, both **PY-TFA** and **TPA-TFA** are highly fluorescent with a quantum yield of ~63%, while fluorescence quantum yield of **ANT-TFA** is as low as 3%. Therefore, for both **TPA-TFA** and **PY-TFA** molecules exist strong intramolecular charge transfer, and the CT state are highly fluorescent. In film state, **PY-TFA** emits strong yellow fluorescence which is also the longest among the three probes and red-shifted 100 nm relative to that in solution. As comparison, **TPA-TFA** shows a broad emission peak at 525 nm and presents a blue shift of 18 nm relative to that in THF. The emission of **ANT-TFA** is very weak under the excitation of mobile UV-lamp with a wavelength 365 or 254 nm. As can be seen in Figure 2c，**ANT-TFA** has a very weak CT band compared with the other two probes, which may be the main reason for its very weak fluorescence. Compared with that of TPA-TFA, such a big red shift emission of **PY-TFA** relative to that in solution could be easily interpreted, because pyrenyl derivatives are known in that they tend to form excimer or aggregation in solid state due to their rigid and big aromatic ring resulting in the longest emission. However, TPA has a pyramidal structure and tends to prevent a face to face π-π stacking, the big steric hinderance may make TPA structure much distorted, hence the emission spectra slightly blue shifted.

To prove the charge transfer characteristic of the spectra, we carried out the solvent dependent absorption and emission spectral studies of all the three probes. The results were summarized in Table S2, S3 and Figure S11~S13. It shows that **PY-TFA** and **TPA-TFA** have such solvatochromism behaviour while **ANT-TFA** has not, and according to Lippert-Mataga

equation,[23, 24] the dipole moment difference of their excited state and basic state could be calculated 0, 2.4 and 6.5 D for **ANT-TFA**, **PY-TFA** and **TPA-TFA**, respectively, clearly demonstrating a charge transfer character of the above mentioned
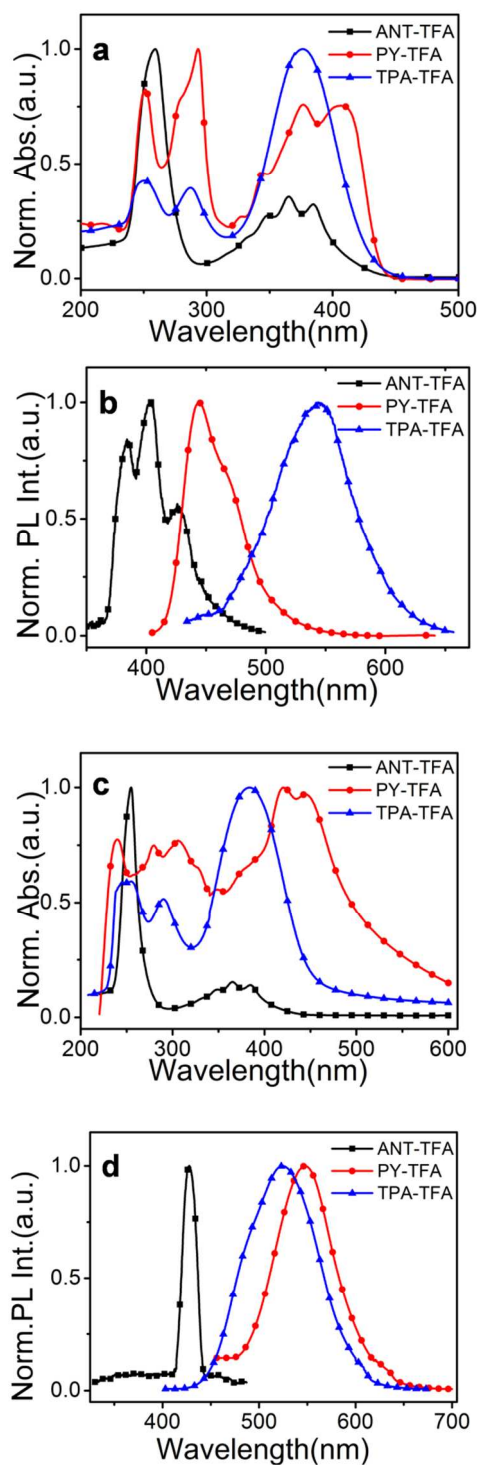5　absorption or emission band for **PY-TFA** and **TPA-TFA**.

Figure 2. The normalized UV-vis absorption and emission spectra of **ANT-TFA**, **PY-TFA**, **TPA-TFA** in solutions(a,b) and films(c,d).

To find why **PY-TFA** and **TPA-TFA** demonstrated such an efficient charge transfer, quantum chemical calculations were

performed by Materials Studio based on DMol3 program. Figure 3 presents the optimized molecular structure in a sideview. As can be seen, for **PY-TFA**, the pyrenyl rings, carbonyl and the trifluoromethyl unit are in a plane contributing to a very efficient charge transfer. The rather planar structure is also responsible for significantly red shifted emission due to the formation of excimer or aggregation in solid state. For **TPA-TFA**, only the phenyl ring connected with TFA unit and the trifluoromethyl unit lie in a plane, although there is a nitrogen atom in it, the charge transfer will not as effective as **PY-TPA**. The nonplanar structure is also in agreement with its short wavelength emission due to unfavorable packing in solid state. For **ANT-TPA**, both carbonyl and the trifluoromethyl unit deviate from the anthracene plane resulting in the poorest charge transfer among them. Figure 4 presents the charge distribution of the HOMO and LUMO level of **TPA-TFA**. As can be seen, the electron are delocalized in the whole molecule in its HOMO, and localized on TFA unit and the phenyl ring connected with it in its LUMO demonstrating a characteristic of charge transfer. Same results could be found for the other two probes (Figure S14, S15). These data well support their spectral data including the CT absorption band and the emission wavelength. The relative spacial position of the aromatic unit and TFA unit is responsible for the absorbance of the CT band, which, in combination with the nature of the aromatic unit including electron donating ability, rigidity, will determine the reactivity and the selectivity to the analytes. For amine sensing, the CT band will be changed due to the influence of the electron-donating amine, and the strength change could reflect the reactivity of the probes and the amines.

The cyclic voltammetry curves of **ANT-TFA**, **PY-TFA**, **TPA-TFA** were shown in Figure S16~S18. It could be seen that **ANT-TFA** showed irreversible p-doping/dedoping and n-doping/dedoping, **PY-TFA** gave irreversible p-doping/dedoping but reversible n-doping/dedoping and **TPA-TFA** presented both reversible p- and n-doping/dedoping. The results also suggest that the TFA is a nice unit for a reversible sensing and the character of the aromatic units will highly influence the electrochemical properties of the probes.
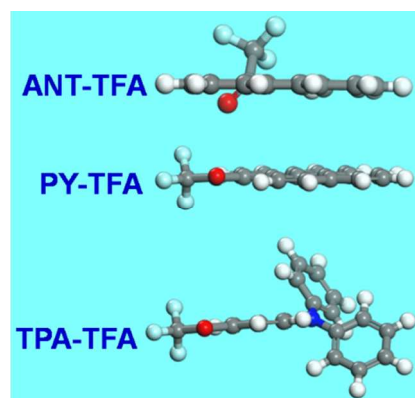

Figure 3. The molecular conformation side view of **ANT-TFA**, **PY-TFA**, **TPA-TFA**.

ARTICLE TYPE

Table1.Optical and electrochemical properties of **ANT-TFA**,**PY-TFA** and **TPA-TFA**.

	Abs^a,λmax/nm		PL^a,λmax/nm						
	Solution	Film	Solution	Film	HOMO/eV	LUMO/eV	ΔE/eV	Φ^b	lgε$_{max}$
ANT-TFA	258(s),365(w),385(w)	254	403	440	-5.95	-3.68	2.27	0.031	3.81
PY-TFA	251(s),293(s),376(s),410(s)	420	444	545	-5.98	-3.72	2.30	0.626	4.21
TPA-TFA	249(w),287(w),377(s)	383	543	525	-5.89	-3.35	2.54	0.632	4.45

^{a}Samples are measured in THF solutions or films by spin-coating its THF solution (4 mg/mL) on the quartz plate (10 ×20 mm).
^{b}The fluorescence quantum yields of **ANT-TFA**,**PY-TFA**,**TPA-TFA**in a THF dilute solution were measured using a THF dilute solution of 9,10-
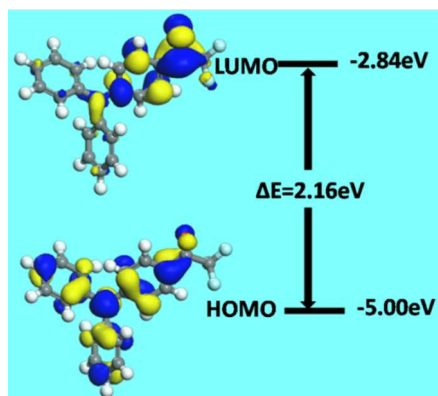5 diphenylanthracene in THF solution as the standard.

Figure 4. Optimized molecular structure and molecular orbitals of **TPA-TFA**.

10

3.2Sensory properties

Figure 5 shows the photos of the **ANT-TFA**, **PY-TFA**, **TPA-TFA** films excited by UV lamp at a wavelength of 365 nm after
15 100 s exposure in air and several saturated organic amine vapour. Clearly, in primary alkyl amines (*n*-propylamine and *n*-hexylamine) and secondary alkyl amines (diethylamine and dipropylamine), the emission of **PY-TFA** will be changed from yellow colour to blue or be quenched, but in aniline, no
20 detectable change is observed. While for **TPA-TFA**, the yellow-greenish emission changed to blue in primary alkyl amine, partly quenched in secondary alkyl amine and completely quenched in aniline. And due to very weak fluorescence of **ANT-TFA**, it is not suitable for such detection. Aside from amines mentioned
25 above, these three probes are also applicable for other primary and secondary amines, such as *iso*butylamine, *n*-octylamine, di*iso*propylamine, dipentylamine, *o*-toluidine (Figure S19). The responses of **PY-TFA** and **TPA-TFA** films to aliphatic tertiary amine were also checked, but no response could be detected after
30 a 100 s exposure (Figure S20). Based on the experiments, two

points could be obtained. On the one hand, **TPA-TFA** showed a higher reactivity than **PY-TFA** since it even could react with aniline, the lower reactivity of **PY-TFA** is related to its more effective intramolecular charge transfer. On the other hand, the
35 reactivity of different amines are quite different, the relatively weak electrophilicity of aniline comes from the electron delocalization of nitrogen to the phenyl ring, and the reactively of tertiary amine results from its large steric hindrance.
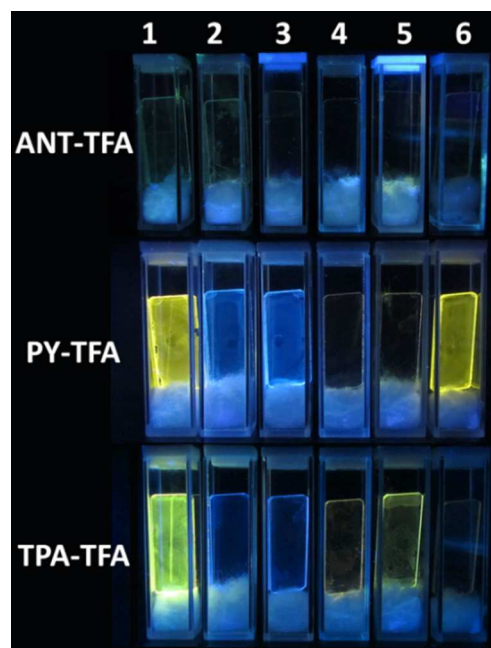

40 Figure 5. **ANT-TFA**, **PY-TFA**, **TPA-TFA** films excited by UV lamp 365 nm after 100s exposure in air and several saturated organic amine vapour (1 air, 2 *n*-propylamine, 3 *n*-hexylamine, 4 diethylamine, 5 dipropylamine, 6 aniline).
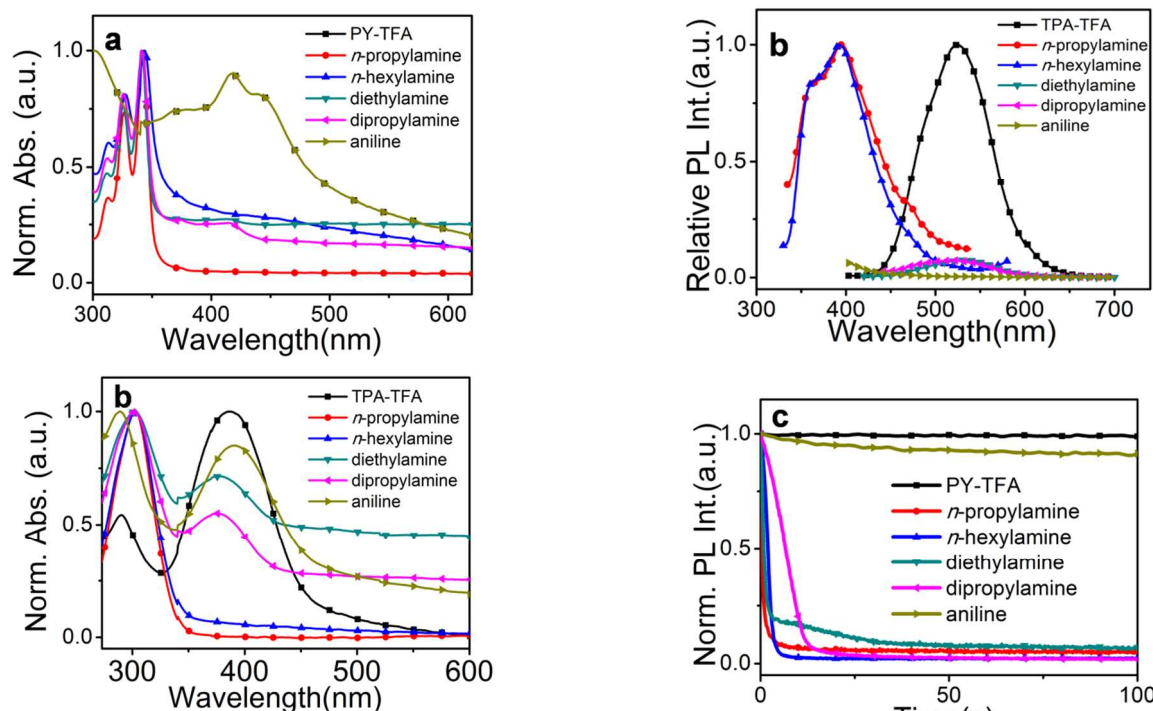
Figure 6. The normalized UV-Vis spectra of **PY-TFA** (a) and **TPA-TFA** (b) films in the presence of different saturated amines vapour.

5   Figure 6 presents the absorption spectra of **PY-TFA** and **TPA-TFA** films before and after exposure to the amines vapour. For **PY-TFA**, except in aniline, the CT band ranging from 350~600 nm disappeared in alkyl primary and secondary amines with the appearance of several new absorption band below 350 nm and

10 with fine structure. And for **TPA-TFA**, in primary alkyl amines, the CT band peaked at ~400 nm disappeared while the band peaked at ~300 nm was enhanced. As comparison, in secondary amine and aniline, the band at ~400 nm showed a slight wavelength shift and decreased absorbance, which is lower than

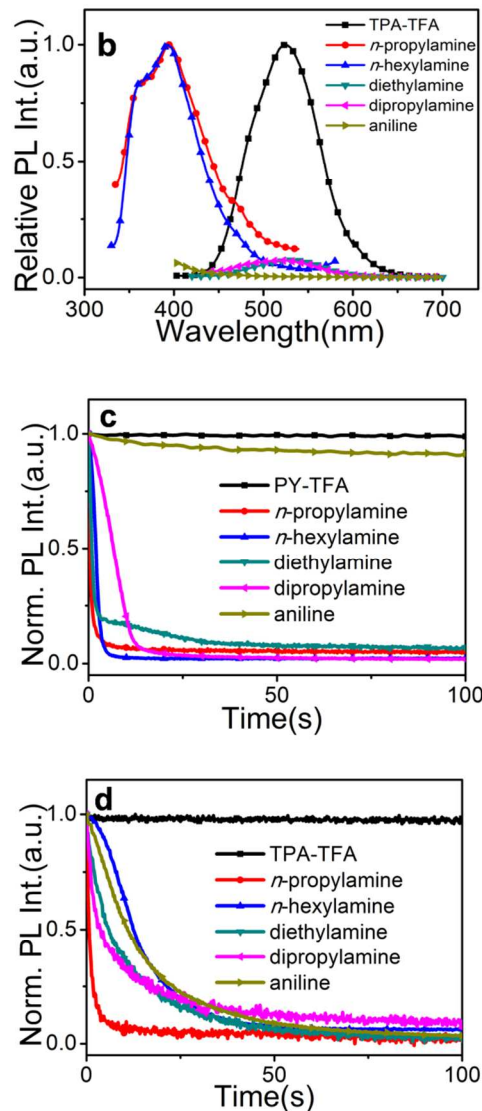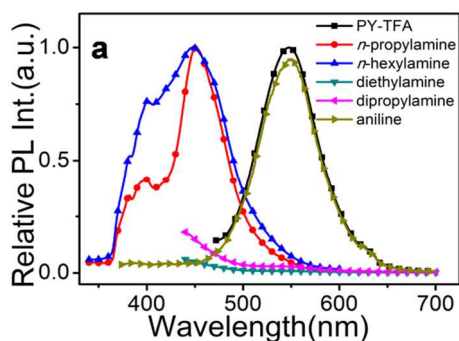15 that at ~300 nm compared with its pristine film.

20

Figure 7.Changes of **PY-TFA** and **TPA-TFA** films after 100s exposure in air and several saturated organic amine vapour: (a) (b) spectral changes, (c) (d) stability and sensing properties, the emission intensities of **PY-TFA** and **TPA-TFA** were monitored at 545nm and 525 nm, respectively.

25   As mentioned earlier, trifluoroacetyl group will be converted into a hemiaminal via reversible chemical reaction with amines, The fluorescence changes of **PY-TFA** and **TPA-TFA** in different amines were monitored by fluorescencespectraas shown in Figure 7a and 7b. For **PY-TFA**, the emission maximum will be changed

30 from 545 to 452 nm upon exposure to the saturated primary amine vapour, quenched in secondary amine vapours, and showed minor intensity change in aniline vapour after 100 s' exposure. As compared, for **TPA-TFA**, the emission maximum will be changed from 525 to 394 nm in primary amine, quenched

35 in both secondary amine and aniline vapour. Figure 7c and 7d present the emission maxima change of **PY-TFA** and **TPA-TFA** in amines with time. Within 25 s, the quenching rate of PY-TFA reached up to 95% in primary and secondary alkyl amines, but in aniline, only 8% was quenched. As for **TPA-TFA**, within 50 s,

40 the emission could be quenched by primary, secondary alkyl amines and aniline. The time curves of **PY-TFA** and **TPA-TFA** displayed very fast and efficient response to amine vapour, which

is in conformity with the phenomenon of Figure 5.

Based on the results, a possible sensing mechanism for the two probes was proposed. In primary alkyl amines, the reversible reaction between the amines and TFA unit could inhibit the intramolecular charge transfer and produce a blue shifted emission after the amines exposure for both **PY-TFA** and **TPA-TFA**. In secondary amines, for **PY-TFA**, the reversible reaction still occurs judging from the disappeared CT band (Figure 6a) at ~400 nm, but after that, since the secondary amine (for example, E_{HOMO}(dibutylamine)=-5.6 eV) has a higher HOMO level than that of **PY-TFA**(E_{HOMO}=-5.98 eV) (Figure S21), it could further experience a photoinduced electron transfer (PET) to the HOMO of the excited **PY-TFA** molecules resulting in a fluorescence quenching (primary amine cannot do that for its lower HOMO, E_{HOMO}(n-hexylamine)=-6.12 eV).[25] And for **TPA-TFA** (E_{HOMO}=-5.89 eV), the reversible reaction only partly exists judging from the decreased CT absorption band, and the PET should also be the reason of the effective fluorescence quenching. In aniline, due to its poor reactivity, there is no reaction between **PY-TFA** and aniline, and no fluorescence quenching occurs. However, **TPA-TFA** still could partly reacts with it based on the decreased CT band, followed by a PET resulted fluorescence quenching (E_{HOMO}(aniline)=-5.26 eV).[25] According to these results, two points could be drawn. Firstly, different aromatic units could lead to a much different reactivity. Secondly, the reactivity and the energy level of the amines is critical for the selectivity.

The reversibility of **TPA-TFA** film to n-propylamine vapour was demonstrated in Figure 8 as an example. ~95% of its initial fluorescence intensity could be quenched and recovered within 15 s' exposure to n-propylamine vapour and neat air in sequence. The recovery curves of secondary amines and aniline were displayed on Figure S22 and S23. Clearly, it exhibits excellent reversibility upon consecutive and alternative exposures to amine and air. It proves directly that the reaction of trifluoroacetyl with amine is reversible and very efficient.
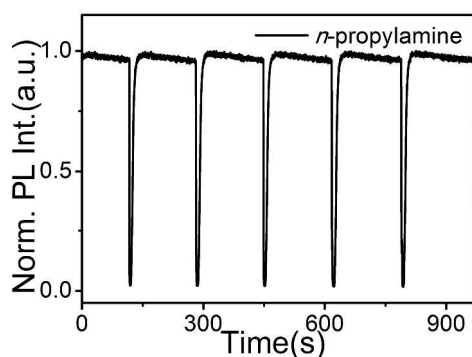

Figure 8. Repeatability of **TPA-TFA** film exposed to n-propylamine vapour, the emission intensity was monitored at 525 nm.

By stepwise dilution of the amine vapour, the fluorescence intensity of **TPA-TFA** films versus different concentrations of amine vapour (Figure S24~S28) was monitored, same experiment was also carried out based on **PY-TFA** film. According to the saturated vapour pressure of different amines at 20°C (Table S4), if the SNR of the fluorescence instrument was considered as 1‰, an estimated detection limits of **TPA-TFA** and **PY-TFA** are at ppm-ppb level (Table S5). The fluorescence quenching efficiency

of **TPA-TFA** as a function of the vapour pressure of aniline was illustrated in Figure 9 as an example. The fluorescence quenching data is well-fitted by the Langmuir equation and the detection limit could be speculated to 0.23 ppb according to the fitted curve. Generally speaking, **TPA-TFA** showed much better sensitivity than **PY-TFA** except for n-hexylamine. For instance, the lowest detection limit for diethylamine is 0.17 ppb, which is far less of the IDLH (Immediately Dangerous to Life or Health) concentration. And for aniline, the detection limit of 0.23 ppb is also much lower than its IDLH concentration of 100 ppm. The detection limit of **PY-TFA** for diethylamine can also be as low as 2.04 ppm, much lower than its IDLH concentration of 200 ppm. Taken together, **TPA-TFA** and **PY-TFA** could serve as a sensitive, simple, rapid response sensing materials in the fluorescent film sensors for real-time monitoring of amines, and due to a relatively larger reactivity of **TPA-TFA**, the detection limit of **TPA-TFA** is lower than **PY-TFA**.
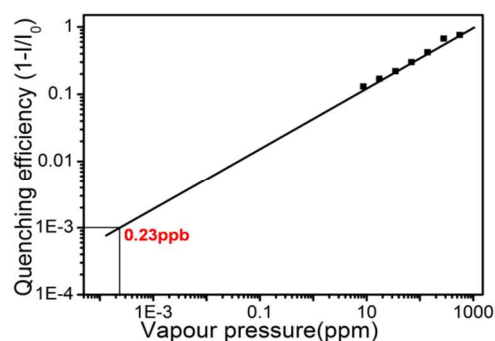

Figure 9. The fluorescence quenching efficiency (1-I/I0) of **TPA-TFA** as a function of the vapour pressure of aniline, data (error 5%) fitted with the Langmuir equation.

Due to the complexity of the live environment, we further examined the sensing performance of **TPA-TFA** in the mixed amines including primary and secondary alkyl amines and aniline (Figure10). The experimental result revealed that upon contacting with mixed amines, the maximum emission peak of **TPA-TFA** blue shifted to 362 nm and 90% is quenched at 25 s at its emission maximum (525 nm). But for further differentiating the amines, it should be used together with **PY-TFA** considering that **PY-TFA** gives no response to aniline, and the emission colour of **TPA-TFA** will be different under the existence of primary alkyl amine and secondary amine.
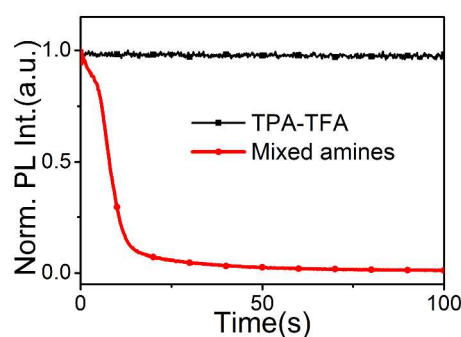

Figure 10. The stability and sensing properties changes of **TPA-TFA** film after 100s exposure in air and mixed amine vapour, the emission intensity was monitored at 525 nm.

4 Conclusion

In summary, we have synthesized fluorescent trifluoroacetyl-substituted aromatic compounds for quick, sensitive and reversible organic amine vapour detection. By selecting suitable aromatic substituent, the reactivity and fluorescent properties could be tuned with it to afford an efficient amine probe. **PY-TFA** shows intense luminescence and could be rapid and sensitive to detect aliphatic primary and secondary amine vapour except aniline vapour. While **TPA-TFA** is proved to be a simple but effective probe for detecting aliphatic primary amines, aliphatic secondary amines and aniline. The detection limit could be as low as 0.17 ppb for diethylamine and 0.23 ppb for aniline. The probes are characteristic of simple, rapid response, reversibility and high sensitivity is capable for real-time monitoring of organic amines. The probe design strategy is very useful for such probe development on real-time, on site and efficient monitoring of pollutants detection.

Acknowledgements

Notes and references

[a]State Key Lab of Transducer Technology, Shanghai Institute of Microsystem and Information Technology, Chinese Academy of Sciences, Changning Road 865, Shanghai 200050, China.
E-mail:hqg@mail.sim.ac.cn;jgcheng@mail.sim.ac.cn;Fax:+86-21-62511070-8934; Tel: +86-21-62511070-8967.
[b]University of the Chinese Academy of Sciences, Yuquan Road 19, Beijing,100039, China

†Electronic Supplementary Information (ESI) available: Chemical reaction of trifluoroacetyl group with amines, ^{1}H and ^{13}C NMR of **ANT-TFA**, **PY-TFA**, **TPA-TFA**, DMol3 optical absorption spectra and optimized molecular structure and molecular orbitals of **ANT-TFA** and **PY-TFA**, detail methodology and parameters of DMol3, CV curves, Lippert-Mataga equation parameters, **ANT-TFA**, **PY-TFA**, **TPA-TFA** films excited by UV lamp 365 nm after 100 s' exposure in air and aliphatic tertiary amine vapour, fluorescence intensity of **TPA-TFA** films exposed to different concentrations of amine vapour, saturated vapour pressure of different amines at 20°C, detection limit of **PY-TFA** and **TPA-TFA**. See DOI: 10.1039/b000000x/

1. T. Gao, E. S. Tillman and N. S. Lewis, *Chem. Mater.*, 2005, **17**, 2904-2911.
2. J. M. Landete, B. de las Rivas, A. Marcobal and R. Muñoz, *J. M. Landete et al.*, 2007, **117**, 258-269.
3. A. P. De Silva, H. N. Gunaratne, T. Gunnlaugsson, A. J. Huxley, C. P. McCoy, J. T. Rademacher and T. E. Rice, *Chem. Rev.*, 1997, **97**, 1515-1566.
4. W. P. Ambrose, P. M. Goodwin, J. H. Jett, A. Van Orden, J. H. Werner and R. A. Keller, *Chem. Rev.*, 1999, **99**, 2929-2956.
5. M. Comes, M. D. Marcos, R. Martínez-Máñez, F. Sancenón, L. A. Villaescusa, A. Graefe and G. J. Mohr, *J. Mater. Chem.*, 2008, **18**, 5815.
6. O. A. Egorova, H. Seo, A. Chatterjee and K. H. Ahn, *Org. Lett.*, 2009, **12**, 401-403.
7. Y. Fu, Y. Gao, L. Chen, Q. He, D. Zhu, H. Cao and J. Cheng, *RSC Adv.*, 2014, **4**, 46631-46634.
8. W. Chyan, D. Y. Zhang, S. J. Lippard and R. J. Radford, *PNAS*, 2014, **111**, 143-148.
9. J. Wu, W. Liu, J. Ge, H. Zhang and P. Wang, *Chem. Soc.Rev.*, 2011, **40**, 3483-3495.
10. C. J. Liu, J. T. Lin, S. H. Wang, J. C. Jiang and L. G. Lin, *Sens. Actuators. B*, 2005, **108**, 521-527.
11. D.-S. Kim, Y.-M. Chung, M. Jun and K. H. Ahn, *J. Org. Chem.*, 2009, **74**, 4849-4854.
12. G. Lu, J. E. Grossman and J. B. Lambert, *J .Org. Chem.*, 2006, **71**, 1769-1776.
13. T. Han, J. W. Lam, N. Zhao, M. Gao, Z. Yang, E. Zhao, Y. Dong and B. Z. Tang, *Chem.Commun.*, 2013, **49**, 4848-4850.
14. S. Rochat and T. M. Swager, *Angew. Chem. Int. Ed.*, 2014, **53**, 9792-9796.
15. E. Mertz and S. C. Zimmerman, *J. Am. Chem. Soc.*, 2003, **125**, 3424-3425.
16. S. Korsten and G. J. Mohr, *Chem. Eur. J.*, 2011, **17**, 969-975.
17. H. Iida, M. Miki, S. Iwahana and E. Yashima, *Chem. Eur. J.*, 2014, **20**, 4257-4262.
18. Y. Fu, Q. He, D. Zhu, Y. Wang, Y. Gao, H. Cao and J. Cheng, *Chem.Commun.*, 2013, **49**, 11266-11268.
19. L. Shi, Y. Fu, C. He, D. Zhu, Y. Gao, Y. Wang, Q. He, H. Cao and J. Cheng, *Chem.Commun.*, 2014, **50**, 872-874.
20. G. J. Mohr, C. Demuth and U. E. Spichiger-Keller, *Anal. Chem.*, 1998, **70**, 3868-3873.
21. G. Mohr and U. Spichiger, *J. Mater. Chem.*, 1999, **9**, 2259-2264.
22. G. J. Mohr, *Chem. Eur. J.*, 2004, **10**, 1082-1090.
23. E. Lippert, *Z. Phys. Chem.*, 1956, **6**, 125.
24. E. Von Lippert, *Bull. Chem. Soc. Jpn*, 1956, **29**, 465.
25. Y. Che, X. Yang, S. Loser and L. Zang, *Nano Lett.*, 2008, **8**, 2219-2223.